

Glycine-Induced Synthesis of Vaterite via Direct Aqueous Mineral Carbonation of Flue Gas Desulfurization Gypsum

Xuemin Liu

Jinxi Industries Group Co., LTD

Zhihe Pan

Shanxi University

Huagang Cheng

Shanxi University

Zhien Zhang

West Virginia University

Fangqin Cheng

Shanxi University

Bo Wang (✉ wangbo@ipe.ac.cn)

CAS Institute of Process Engineering <https://orcid.org/0000-0003-4911-8352>

Research Article

Keywords: flue gas desulfurization gypsum, mineral carbonation, CaCO₃, vaterite, glycine

Posted Date: December 6th, 2021

DOI: <https://doi.org/10.21203/rs.3.rs-1050584/v1>

License: © ⓘ This work is licensed under a Creative Commons Attribution 4.0 International License.

[Read Full License](#)

Abstract

Mineral carbonation of flue gas desulfurization gypsum (FGDG) can not only sequester CO₂ to mitigate the greenhouse effect, but also produce CaCO₃ to generate economic benefit. A mixture of calcite and vaterite CaCO₃ was produced by FGDG carbonation in our previous study. Nevertheless, the production of uniform crystalline CaCO₃, especially for vaterite, still maintains a big challenge via carbonation of FGDG. Herein, nearly pure vaterite was synthesized via FGDG carbonation in the presence of glycine was reported firstly. The results show that the content of vaterite increased from 60% to 97% with increasing glycine concentration and then kept a constant value, indicating that glycine can promote the formation of vaterite and inhibit the growth of calcite. Additionally, the investigation of vaterite growth mechanism in the presence of glycine demonstrated that the formation of intermediate, glycinate calcium, played an important role to stimulate the growth of vaterite. This study provides a new insight to produce a high-valued vaterite CaCO₃ during the direct mineral carbonation of FGDG.

1. Introduction

Flue gas desulfurization gypsum (FGDG) is a kind of industrial waste discharged from limestone-gypsum wet desulphurization process, which has led to serious environmental problems due to lack of effective and environmentally friendly disposal methods. For instance, a series of problems including occupying land, polluting water, particle pollution and ecological destruction have been caused due to the ineffective treatment of FGDG (Alvarez-Ayuso et al. 2008; Zhao et al. 2018). However, huge amount of FGDG has been generated worldwide, especially in China (80 Mt, 2017) and USA (30 Mt, 2015) (Walia & Dick 2018; Wang et al. 2021; Tan et al. 2018). Furthermore, the annual production of FGDG was estimated to undergo an increasing tendency in the coming future. Although numerous stacking FGDG causes many environmental or ecological issues, FGDG is a kind of useful resource actually because it contains rich calcium and sulfur element. Consequently, the utilization and management of hazardous FGDG are indispensable way to reduce the pollution and realize the high-efficiency and clean production process.

Recently, mineral carbonation of FGDG to sequester CO₂ has received attentions extensively. This technology is a “win-win” strategy because it can not only achieve CO₂ reduction, but also realize the resource utilization of FGDG to produce toxic-free CaCO₃ and achieve the goal of treating waste with wastes. Synthesis of CaCO₃ by FGDG carbonation presents a high yield and conversion efficiency (Lee et al. 2012). CaCO₃ is important fillers or additives in paper, plastic, food, cosmetics, medical materials and composite functional materials because of its unique characteristics of nontoxicity and harmlessness, biocompatibility, easy fabrication and controllable structure (Konopacka-Łyskawa et al. 2017; Mori et al. 2009; Wang et al. 2018). Therefore, the hazardous FGDG was transformed into eco-friendly CaCO₃ is an alternative strategy to deal with million tons of discarded FGDG thereby reducing its pollution to the natural environment and improve its high value-added.

Generally, CaCO_3 has three anhydrous polymorphs (calcite, aragonite and vaterite), among which calcite shows the highest stability, while aragonite and vaterite are metastable and thermodynamically unstable phases respectively (Zhou et al. 2010). Among of them, vaterite-type CaCO_3 particles show special properties, such as high specific surface area, high solubility, smaller gravity, hierarchical structures and biocompatibility (Beuvier et al. 2011; Tolba et al. 2016; Xu et al. 2014). Thus, vaterite has been extensively applied in many fields (such as coating and ink etc.). Moreover, vaterite is not only a potential material for industries applications, but also the essential component of organism (Konopacka-Łyskawa 2019; Lowenstam & Abbott 1975; Wightman et al. 2018). Consequently, production of vaterite via FGDG carbonation will enhance the competitive of the products and open another gate of clean utilization of FGDG.

Over the past decades, many works have been focused on using FGDG to produce high-valued CaCO_3 by carbonation method. The high-purity CaCO_3 (calcite) particles were synthesized by using the solution which was extracted from the induction period of CaCO_3 during the process of FGDG carbonation (Song et al. 2012). However, the yield of pure calcite is relatively low (about 5% of FGDG) because of the short induction period of CaCO_3 crystallization. To improve the production of pure CaCO_3 (calcite), polyacrylic acid (PAA) was used to prolong the induction time of CaCO_3 crystallization during FGDG carbonation and the yield of calcite was improved to 60% (Song et al. 2016). Moreover, our previous work found that the content of vaterite increased from 60–80% in $\text{CaSO}_4\text{-NH}_3\text{-CO}_2\text{-H}_2\text{O}$ supernatant system due to the ultrasonic induction (Cheng et al. 2016). Nevertheless, the yield of CaCO_3 is relatively low and further improvement on the production of CaCO_3 should be considered. In other work, a mixture of vaterite and calcite was also observed in FGDG suspension carbonation system below 60°C of reaction temperature (Lee et al. 2015). Meanwhile, our previous work shown that a mixture of calcite (40%) and vaterite (60%) was produced via carbonation of FGDG (Wang et al. 2019). Additionally, the study of the formation mechanism of polymorph of CaCO_3 (a mixture of calcite and vaterite) found that impurity of dolomite from the FGDG induce to form calcite due to the dolomite lead to a high local ratio of $\text{Ca}^{2+}/\text{CO}_3^{2-}$ which favors to form calcite. In summary, although high yield of CaCO_3 was obtained through carbonation of FGDG, the carbonation products were still a mixture of vaterite and calcite. Therefore, synthesis of uniform vaterite still face a big challenge via direct aqueous carbonation of FGDG.

Vaterite production has been received more and more attention because of its special properties and intensively application. Generally, the organic/inorganic additives (Kirboga & Öner 2017; Lorenzo et al. 2017), templates (Choi & Kuroda 2012) and ultrasound (Juhász-Bortuzzo et al. 2017; Svenskaya et al. 2016) were used to control the formation of vaterite. Among of them, amino acids as the common additives were used to induce the formation of vaterite. The monodisperse spherical vaterite (CaCO_3) was synthesized using glycine (Gly) in a calcium hydroxide (Ca(OH)_2)-carbon dioxide (CO_2) reaction system at room temperature and atmospheric pressure (Lai et al. 2015). It was illustrated that the complex effects between Gly and Ca^{2+} played a key role in the formation process of monodisperse spherical vaterite. Luo et al. (Luo et al. 2015) investigated the role of aspartic acid (Asp) on synthesis of spherical vaterite in the

Ca(OH)₂-CO₂ reaction system. Vaterite is induced through the intermediate chelated by Asp and Ca(OH)₂, and then Asp is adsorbed on the surface of vaterite by chelation, preventing the metastable vaterite from transforming to calcite via a dissolution-recrystallization process (Luo et al. 2015). Jiang and co-workers reported that the chiral acidic amino acids induce chiral hierarchical structure in vaterite by using aspartic acid and glutamic acid (Jiang et al. 2017). In other work, the crystallization of vaterite was proceeded via a pseudomorphic transformation of ACC nanospheres at high poly(aspartic acid) concentrations (Zou et al. 2017). Also, it was reported that L-Tyrosine (L-Tyr), DL-Aspartic Acid (DLAsp) and L-Lysine induced the formation of vaterite (Xie et al. 2005). Shivkumara et al. (Shivkumara et al. 2006) synthesized of vaterite CaCO₃ by direct precipitation using glycine and L-alanine as directing agents. It was found that glycine or any amino acid having isoelectric point around pH=6 can be used for precipitation of vaterite CaCO₃. Tong et al. (Tong et al. 2004) fabricated the vaterite by using L-aspartic acid (L-Asp). It was indicated that vaterite can be formed in the presence of L-Asp and it is able to maintain its stability compared with the crystals formed in the absence of L-Asp. Kai et al. (Kai et al. 2002) indicated that noncharged and polar amino acids and those of the acidic ones in CaCO₃ precipitates tended to stabilize the vaterite phase, and the vaterite content in CaCO₃ precipitates is correlated to the concentration of amino acids in the precipitates. Gan et al. (Gan et al. 2017) investigated the effect of glycine on the growth of CaCO₃ in alkaline silica gel. It was shown that spherical vaterite particles formed in alkaline silica gel concomitantly together with dumbbell shaped calcite particles when the initial concentration of glycine was high enough (10 mg/mL, 20 mg/mL).

Hence, the aim of this work is to synthesize vaterite via direct aqueous carbonation of FGDG. Herein, the glycine was chosen as the additives to investigate the effect of glycine on the polymorph CaCO₃ during the FGDG carbonation. Nearly pure vaterite was produced at the optimal conditions. The formation mechanism of vaterite via FGDG carbonation in the presence of glycine was also explored. The research finding might find a new approach to manage the FGDG and enhance its added high-value.

2. Experimental

2.1. Materials

The flue gas desulfurization gypsum (FGDG) was obtained from Taiyuan Iron & Steel (group) Co., LTD. (Shanxi, China) and was screened to 200 meshes for use. Ammonia solution (NH₄OH, 25 wt%, density: 0.9 g/mL) was purchased from Tianjin Damao Chemical Reagent Factory. The purity of CO₂ is 99.99%. Deionization (DI) water was provided by our lab. All the experiments were conducted at room temperature (25°C) and atmospheric pressure.

2.2. Synthesis procedure of vaterite in the presence of glycine

In general experiments, glycine (5, 10, 15, 20, 40 wt%, mass ratio of glycine to FGDG) was dispersed in the FGDG suspension containing ammonia which was prepared according to our previous work (Wang et al.

2019). Then the suspension was stirred using magnetic stirring at a constant speed of 450 rpm. After stirring for 10 mins, CO₂ gas (200 mL/min) was bubbled into the bottom of the reactor (glass reactor, diameter: 50 mm, height: 1300 mm) under magnetic stirring (450 rpm) for 1 h. The obtained samples were isolated by filter and washed with DI water at least three times, and dried at 60°C for 24 h before characterization. Meanwhile, the precipitated particles were collected during CO₂ bubbling to analyze the behavior of precipitation reaction.

2.3 Carbonation products of glycinate calcium

In order to prove glycinate calcium (Ca(NH₂CH₂COO)₂) plays a critical role in vaterite growth, Ca(NH₂CH₂COO)₂, ammonia and CO₂ were used as reactants to conduct the carbonation. Analytical pure Ca(NH₂CH₂COO)₂ (2 g), ammonia solution (11 mL) were added to 91 mL DI water to prepare the Ca(NH₂CH₂COO)₂ suspension. After stirring of 10 min, CO₂ (200 mL/min) was injected into above suspension to react. After 30 min of reaction, the product was washed with DI water for three times, filtered and dried at 60°C for 24 h before characterization.

2.4. Characterization

The phase composition of the samples was analyzed by XRD (Bruker D2 Advance with a Cu Kα source at 30 kV and 10 mA) with the scanning scope (2θ) from 5° ~ 80° under the speed of 0.02° s⁻¹. Jade 5.0 was used to identify the minerals components of the samples. The content of each CaCO₃ polymorph was calculated from their characteristic XRD peak intensities by using the following equations [23].

$$\frac{I_C^{104}}{I_V^{110}} = 7.691 \frac{X_C}{X_V} \quad (1)$$

$$X_V + X_C = 1 \quad (2)$$

Herein, X_C: molar fractions of calcite and X_V: molar fractions of vaterite. I_C¹⁰⁴: intensities of the peaks of 104 plane of calcite and I_V¹¹⁰: intensities of the peaks of 110 plane of vaterite.

Fourier transform infrared spectra (FTIR) measurements were performed on a Perkin-Elmer 1730 FTIR Spectrometer having a resolution of 2 cm⁻¹ to characterize the structure of samples. Pressed pellets of sample diluted with potassium bromide (2 mg in 300 mg) were prepared and were used for analysis. The morphology of precipitated CaCO₃ samples was observed by SEM (JSM-IT500HR, Japan) under the accelerating voltage of 3 kV. Before the test, a thin layer of gold was coated onto the samples to enhance the conductivity via an ion sputtering apparatus (JEOL-JFC-1600). Furthermore, the element composition of the sample was detected by energy dispersive X-ray (EDS). The simultaneous thermal analysis of thermogravimetry and differential scanning calorimetry (TG-DSC) were conducted on the NETZSCH STA449-F5 with a heat rate of 10°C/min in air atmosphere from 50 to 1100°C. Electrospray ionization

mass spectrometry (ESI-MS) was used to obtain the molecular weight of the intermediate with a Thermo Scientific Q Exactive (Thermo Fisher Scientific, America).

3. Results And Discussion

3.1. Effect of glycine concentration on CaCO₃ polymorphs

In this work, the influence of glycine concentration on CaCO₃ precipitation via carbonation of FGDG was investigated. The XRD patterns of the carbonation products obtained with different glycine concentration are shown in Fig. 1a. It was found that a mixture of calcite and vaterite are obtained in the presence of glycine. However, the diffraction peak intensity of vaterite gradually increased and calcite diffraction peak intensity decreased. In order to quantitatively assess the effect of glycine on the polymorph of CaCO₃, the content of vaterite and calcite in samples was calculated according to Eqs. 2 and 3 (Fig. 1b). As shown in Fig. 1b, the content of vaterite was about 60% in the absence of glycine, while the content of vaterite gradually increased from 60–97% with increasing the glycine concentration up to 20 wt% and then kept a constant value with adding more glycine. Correspondingly, the content of calcite decreases first and then reach a platform with ~3% calcite.

Further, all carbonation products obtained at different concentration of glycine were analyzed by SEM (Fig. S1). The as-prepared samples obtained in the absence of glycine shown sphere-like and rhombohedral particles structure (Fig. S1a), which are similar with our previous result (Wang et al. 2019). However, the sphere-like vaterite gradually increased with increase of glycine concentration, and finally vaterite was dominated phase (Fig. S1b-f). The SEM images further revealed that these microspheres were composed of the aggregation of numerous primary nanoparticles (Fig. S1e-f). Many vaterite microspheres were observed to be interconnected with each other demonstrating there were a tendency of agglomeration or clustering between vaterite particles. Besides, the carbonation products were analyzed by FTIR. With the increase of the concentration of glycine, the characteristic peak of calcite at 712 cm⁻¹ gradually weakened, and the characteristic peak of vaterite (745 cm⁻¹) gradually increased (Fig. S2). The above results confirm that the content of vaterite in carbonation products increase with glycine concentration showing that glycine indeed promote the formation of vaterite and inhibit the growth of calcite.

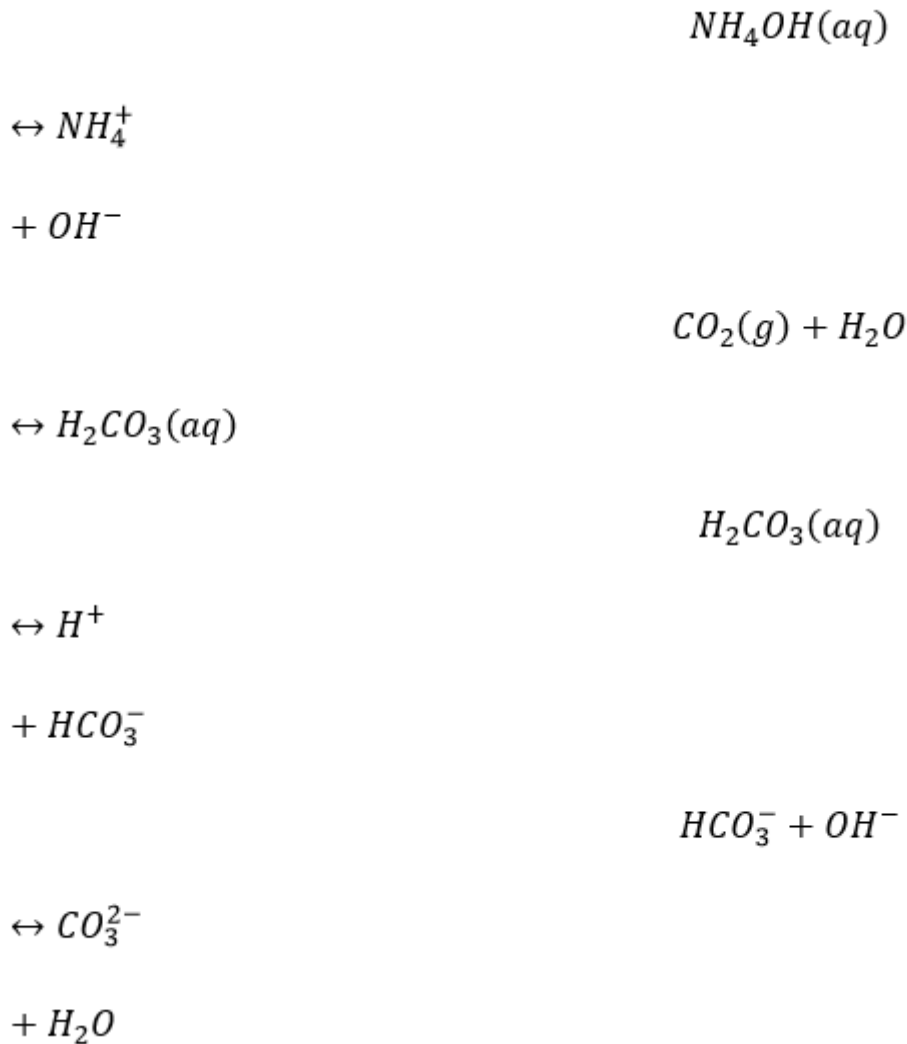
Based on the above result, nearly pure vaterite CaCO₃ was generated with 20 wt% glycine, which was analyzed further by TG-DSC. Fig. S3 shows the TG-DSC curve of carbonation product at the glycine concentration of 20 wt%. TG curve has three temperature ranges of weight loss at 50–200°C, 200–600°C and 600–850°C were ascribed to water evaporation, glycine decomposition and CaCO₃ decomposition respectively. For DSC curve, the endothermic peaks near 100°C and 782°C are due to water evaporation and CaCO₃ decomposition. The exothermic peak near 498°C is due to the phase transformation of vaterite to calcite under high temperature. The TG results further showed that there was a small amount

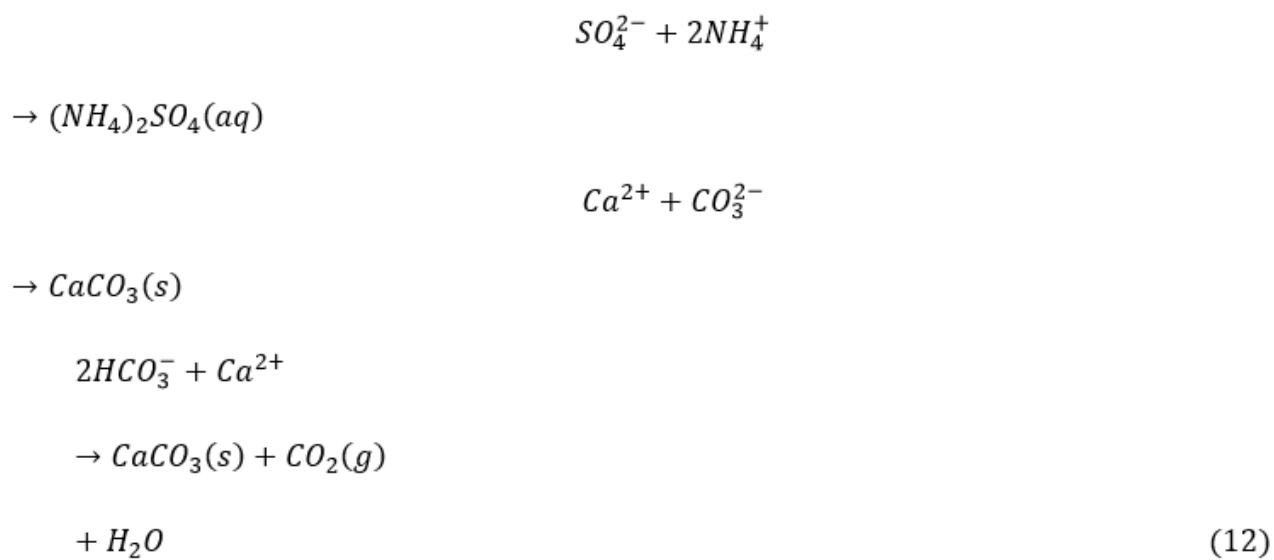
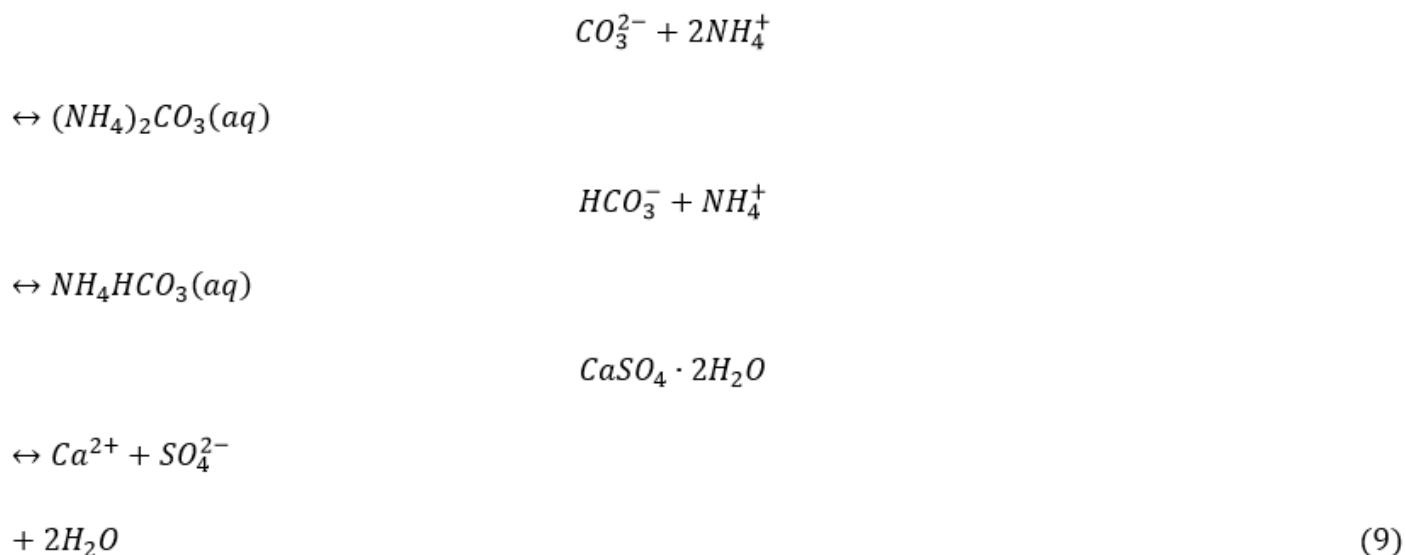
of glycine in CaCO₃ products, which could stabilize the metastable vaterite and prevent it from transforming into calcite (Lai et al. 2015; Luo et al. 2015).

3.2. Mechanism of glycine on precipitated CaCO₃ polymorph

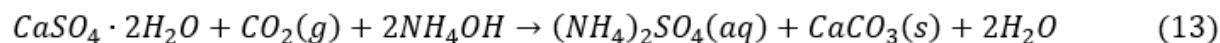
To understand the influence of glycine on CaCO₃ polymorphs, the precipitation process of CaCO₃ was analyzed without glycine. The FGDG carbonation reaction was divided into four main stages: gaseous, liquid, and solid phases were involved, leading to a number of chemical reactions (Lu et al. 2016; Song et al. 2012): (1) absorption of gas CO₂ in the ammonia solution, (2) formation of ammonium (bi)carbonate, (3) chemical reaction between ammonium (bi)carbonate and gypsum, and (4) precipitation of CaCO₃.

The relevant reactions are shown as follow:

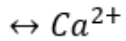
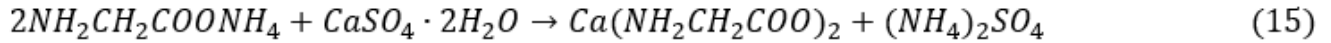
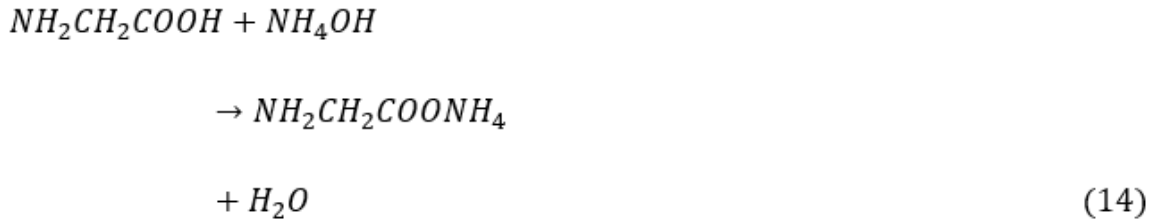




The whole process can be expressed:



As shown in Fig. 1b, a mixture of vaterite (60%) and calcite (40%) was obtained via FGDG carbonation without glycine. However, nearly pure vaterite was generated at 20 wt% glycine (Fig. b). Hence, the assumption that a series of complex reactions might be occurred after adding the glycine was proposed. Firstly, glycine will react with NH_4OH to form ammonium glycinate ($NH_2CH_2COONH_4$) according to the theory of acid-base reaction (Eq. 14). Then, the resulting $NH_2CH_2COONH_4$ further combined with FGDG ($CaSO_4 \cdot 2H_2O$) to form $Ca(NH_2CH_2COO)_2$ and ammonium sulfate ($(NH_4)_2SO_4$) based on the double decomposition reaction due to the low solubility of $Ca(NH_2CH_2COO)_2$ (Eq. 15). At the same time, $Ca(NH_2CH_2COO)_2$ is a kind of complex which was partial ionized based on the reaction of Eq. 16.



In order to prove this assumption that the $\text{Ca}(\text{NH}_2\text{CH}_2\text{COO})_2$ was formed, the filtrate from separating FGDG suspension containing ammonia with 20 wt% glycine was obtained to analyze by ESI-MS (Fig. 2a). It can be seen clearly from Fig. 2a, the mass to charge ratio of 189.01 is $\text{Ca}(\text{NH}_2\text{CH}_2\text{COO})_2$, indicating that $\text{Ca}(\text{NH}_2\text{CH}_2\text{COO})_2$ as an intermediate was indeed generated. Furthermore, we assumed the intermediate of $\text{Ca}(\text{NH}_2\text{CH}_2\text{COO})_2$ plays critical role in promoting vaterite growth. When CO_2 was injected into the system, the carbonate (CO_3^{2-}) reacts with $\text{Ca}(\text{NH}_2\text{CH}_2\text{COO})_2$ to form vaterite. On the other hand, the CO_3^{2-} react with the dissociative Ca^{2+} to form the calcite. Similar results have been reported that the vaterite was induced through the intermediate chelated by aspartic acid and $\text{Ca}(\text{OH})_2$ (Luo et al. 2015). Our previous work indicated that the impurity of dolomite in the FGDG selectively produce the calcite due to the hydrophilicity and negative surface charge of dolomite (Wang et al. 2019). When the glycine was added into the system, the resulting of $\text{NH}_2\text{CH}_2\text{COONH}_4$ might preferentially react with Ca^{2+} dissolved from the FGDG to reduce the adsorption of Ca^{2+} on the dolomite surface. Consequently, the vaterite content enhanced in the presence of glycine. Additionally, the capability of combining Ca^{2+} might increase with the concentration of glycine. Therefore, the vaterite content also increased with increasing of glycine concentration (Fig. 1b).

In order to prove $\text{Ca}(\text{NH}_2\text{CH}_2\text{COO})_2$ can promote vaterite growth, the carbonation products of $\text{Ca}(\text{NH}_2\text{CH}_2\text{COO})_2$ carbonation were analyzed further (Fig. 2b-c). The results showed that the dominated vaterite and small amount calcite were obtained via carbonation of $\text{Ca}(\text{NH}_2\text{CH}_2\text{COO})_2$. Because of the dissolution equilibrium of $\text{Ca}(\text{NH}_2\text{CH}_2\text{COO})_2$, the solution includes the dissociative Ca^{2+} during the carbonation. The formation of vaterite was ascribed to the $\text{Ca}(\text{NH}_2\text{CH}_2\text{COO})_2$, which provided a local lower $\text{Ca}^{2+}/\text{CO}_3^{2-}$ ratio to form vaterite (Abebe et al. 2015; Chang et al. 2016; Svenskaya et al. 2018). Meanwhile, the reason of formation of calcite might be attributed to the dissociative Ca^{2+} . The above results indicated that $\text{Ca}(\text{NH}_2\text{CH}_2\text{COO})_2$ played an important role in the formation of vaterite.

Glycine indeed promoted the growth of vaterite in the carbonation of FGDG. To further investigate the formation mechanism of vaterite in the presence of glycine, the filtrate obtained by solid-liquid separation of FGDG suspension containing ammonia with glycine (20 wt%) was used to react with CO₂ (200 mL/min). Meanwhile, the pH change of the whole process and the precipitation process were monitored. Fig. 3a depicts the pH of filtrate with CO₂ bubbling time. The initial pH was about 10.5, it then quickly dropped to around 8.5, and finally kept a constant value of 7.5. The XRD patterns of the reaction products between the filtrate and CO₂ at different reaction times is shown in Fig. 3b. Only calcite CaCO₃ was found in the product for reaction of 3 min. However, vaterite was found after 6 min of reaction, calcite was dominated phase. As the reaction going, the diffraction peak intensity of vaterite gradually increased, while the diffraction peak intensity of calcite gradually decreased. Finally, the product was dominated by vaterite after 24 min reaction.

The morphology of the reaction products from the reaction of filtrate with CO₂ at different times was further analyzed (Fig. 3c-h). The results showed that the reaction products were mainly calcite particles accumulated by cubic or hexahedral particles at 3 min (Fig. 3c). Spherical vaterite particles were observed for reaction of 6 min, however, the most of particles were still cubic calcite (Fig. 3d). As the reaction goes on, spherical vaterite particles gradually increased and dominated in products (Fig. 3e-h).

The emergence of CaCO₃ polymorphs could be ascribed to the energy barrier to nucleation, which could be explained by Ostwald's step rule (Lakshminarayanan et al. 2003; Rodriguez-Blanco et al. 2011). The metastable vaterite was generally formed first and then transformed into the thermodynamically most stable calcite. But glycine plays a role like some organic additives could protect the crystal surface of the vaterite by interfacial adsorption and stabilize the unstable phase (Abebe et al. 2015; Fu et al. 2013; Nagaraja et al. 2014). According to TG analysis, there was a weight loss of 2.25 wt % at 200–600°C due to the decomposition of glycine (Fig. 3), further revealing that the resulting CaCO₃ contained a few of glycine. These results indicated that the existence of glycine had a stabilizing effect on the metastable vaterite and suppressed its transition to the calcite.

Based on the above results, the formation mechanism of spherical vaterite in the presence of glycine was proposed. Fig. 4 is the schematic diagram of formation mechanism of vaterite with glycine via FGDG carbonation. Initially, Ca(NH₂CH₂COO)₂ was generated during carbonation (Fig. 2a). Hence, when CO₂ was injected into reaction system, CO₃²⁻ gradually generated at pH=10.5. The CO₃²⁻ increased and combined with Ca²⁺ that bound to H₂NCH₂COO⁻ to form vaterite CaCO₃, which was due to the local higher ratio of CO₃²⁻/Ca²⁺ (Dang et al. 2017; Svenskaya et al. 2017). Meanwhile, a little of calcite was also generated during the carbonation. Before injecting CO₂, the dissociative Ca²⁺ was generated through ionizing Ca(NH₂CH₂COO)₂ based on Eq. 16 and dissolving from FGDG. Once CO₂ was flowed into reaction system, CO₃²⁻ was more likely to generate calcite CaCO₃ with dissociative Ca²⁺ due to its low supersaturation and local higher ratio of Ca²⁺/CO₃²⁻ (Chang et al. 2016; Wang et al. 2019).

4. Conclusions

In conclusion, nearly pure vaterite via direct aqueous mineral carbonation of FGDG in the presence of glycine was synthesized. Moreover, formation mechanism of vaterite was also investigated. The vaterite content increased with glycine concentration and then kept a constant value. The highest content of vaterite was about 97% under the optimal conditions. Glycine can promote the formation of vaterite and inhibit the growth of calcite. The study of formation mechanism of vaterite shows that intermediate of $\text{Ca}(\text{NH}_2\text{CH}_2\text{COO})_2$ and adsorption of glycine on the surface of vaterite are the key factors in the growth of vaterite. The small amount of calcite was ascribed to the free Ca^{2+} bound with CO_3^{2-} . This founding may open new insight to realize the clean, high-efficiency production of vaterite via FGDG carbonation.

Declarations

Acknowledgements

This work was supported by the National Key R&D Program of China (2018YFB0605804) and Xiangyuan County Solid Waste Comprehensive Utilization Science and Technology Project (2018XYSDDYY-10).

Declaration of competing interests

The authors declare that they have no known competing financial interests or personal relationships that could have appeared to influence the work reported in this paper.

References

1. Abebe M, Hedin N, Bacsik Z (2015) Spherical and porous particles of calcium carbonate synthesized with food friendly polymer additives. *Cryst Growth Des* 15:3609–3616. doi: 10.1021/cg501861t
2. Alvarez-Ayuso E, Querol X, Tomás A (2008) Implications of moisture content determination in the environmental characterisation of FGD gypsum for its disposal in landfills. *J Hazard Mater* 153:544–550 doi: 10.1016/j.jhazmat.2007.08.088
3. Beuvier T, Calvignac B, Delcroix GJ, Tran MK, Kodjikian S, Delorme N, Bardeau JF, Gibaud A, Boury F (2011) Synthesis of hollow vaterite CaCO_3 microspheres in supercritical carbon dioxide medium. *J Mater Chem* 21:9757–9761 doi: 10.1039/C1JM10770D
4. Chang R, Choi D, Kim MH, Park Y (2016) Tuning crystal polymorphisms and structural investigation of precipitated calcium carbonates for CO_2 mineralization. *ACS Sustain Chem Eng* 5:1659–1667 doi: 10.1021/acssuschemeng.6b02411
5. Cheng H, Wang X, Wang B, Zhao J, Liu Y, Cheng F (2017) Effect of ultrasound on the morphology of the CaCO_3 precipitated from $\text{CaSO}_4\text{-NH}_3\text{-CO}_2\text{-H}_2\text{O}$ system. *J Cryst Growth* 469:97–105. doi: 10.1016/j.jcrysgro.2016.10.017

6. Choi KM, Kuroda K (2012) Polymorph control of calcium carbonate on the surface of mesoporous silica. *Cryst Growth Des* 12:887–893 doi: 10.1021/cg201314k
7. Dang HC, Yuan X, Xiao Q, Xiao WX, Luo YK, Wang XL, Song F, Wang YZ (2017) Facile batch synthesis of porous vaterite microspheres for high efficient and fast removal of toxic heavy metal ions. *J Environ Chem Eng* 5:4505–4515 doi: 10.1016/j.jece.2017.08.029
8. Fu LH, Dong YY, Ma MG, Yue W, Sun SL, Sun RC (2013) Why to synthesize vaterite polymorph of calcium carbonate on the cellulose matrix via sonochemistry process? *Ultrason Sonochem* 20:1188–1193 doi: 10.1016/j.ultsonch.2013.03.008
9. Gan X, He K, Qian B, Deng Q, Lu L, Wang Y (2017) The effect of glycine on the growth of calcium carbonate in alkaline silica gel. *J Cryst Growth* 458:60–65 doi: 10.1016/j.jcrysgr.2016.11.027
10. Jiang W, Pacella MS, Athanasiadou D, Nelea V, Vali H, Hazen RM, Gray JJ, McKee MD (2017) Chiral acidic amino acids induce chiral hierarchical structure in calcium carbonate. *Nat Commun* 8:1–13 doi: 10.1038/ncomms15066
11. Juhasz-Bortuzzo JA, Myszka B, Silva R, Boccaccini AR (2017) Sonosynthesis of vaterite-Type calcium carbonate. *Cryst Growth Des* 17:2351–2356 doi: 10.1021/acs.cgd.6b01493
12. Kai A, Fujikawa K, Miki T (2002) Vaterite stabilization in CaCO₃ crystal growth by amino acid. *Jpn J Appl Phys* 41:439–444 doi: 10.1143/jjap.41.439
13. Kirboga S, Öner M (2017) Investigating the effect of ultrasonic irradiation on synthesis of calcium carbonate using Box-Behnken experimental design. *Powder Technol* 308:442–450 doi: 10.1016/j.powtec.2016.11.042
14. Konopacka-Łyskawa D (2019) Synthesis methods and favorable conditions for spherical vaterite precipitation: a review. *Crystals* 9:223 doi: 10.3390/cryst9040223
15. Konopacka-Łyskawa D, Kościelska B, Karczewski J (2017) Controlling the size and morphology of precipitated calcite particles by the selection of solvent composition. *J Cryst Growth* 478:102–110 doi: 10.1016/j.jcrysgr.2017.08.033
16. Lai Y, Chen L, Bao W, Ren Y, Gao Y, Yin Y, Zhao Y (2015) Glycine-mediated, selective preparation of monodisperse spherical vaterite calcium carbonate in various reaction systems. *Cryst Growth Des* 15:1194–1200 doi: 10.1021/cg5015847
17. Lakshminarayanan R, Valiyaveetil S, Loy GL (2003) Selective nucleation of calcium carbonate polymorphs: role of surface functionalization and poly (vinyl alcohol) additive. *Cryst Growth Des* 3:953–958 doi: 10.1021/cg034022j
18. Lee MG, Jang YN, Ryu KW, Kim W, Bang JH (2012) Mineral carbonation of flue gas desulfurization gypsum for CO₂ sequestration. *Energy* 47:370–377 doi: 10.1016/j.energy.2012.09.009
19. Lee MG, Ryu KW, Chae SC, Jang YN (2015) Effects of temperature on the carbonation of flue gas desulphurization gypsum using a CO₂/N₂ gas mixture. *Environ Technol* 36:106–114 doi: 10.1080/09593330.2014.938126

20. Lorenzo FD, Burgos-Cara A, Ruiz-Agudo E, Putnis CV, Prieto M (2017) Effect of ferrous iron on the nucleation and growth of CaCO_3 in slightly basic aqueous solutions. *Crystengcomm* 19:447–460. doi: 10.1039/C6CE02290A
21. Lowenstam HA, Abbott DP (1975) Vaterite: a mineralization product of the hard tissues of a marine organism (Ascidacea). *Science* 188:363–365 doi: 10.1126/science.1118730
22. Lu SQ, Lan PQ, Wu SF (2016) Preparation of nano- CaCO_3 from phosphogypsum by gas–liquid–solid reaction for CO_2 sorption. *Ind Eng Chem Res* 55:10172–10177 doi:10.1021/acs.iecr.6b02551
23. Luo J, Kong F, Ma X (2015) Role of aspartic acid in the synthesis of spherical vaterite by the $\text{Ca}(\text{OH})_2$ – CO_2 reaction. *Cryst Growth Des* 16:728–736 doi:10.1021/acs.cgd.5b01333
24. Mori Y, Enomae T, Isogai A (2009) Preparation of pure vaterite by simple mechanical mixing of two aqueous salt solutions. *Mater Sci Eng: C* 29:1409–1414 doi: 10.1016/j.msec.2008.11.009
25. Nagaraja AT, Pradhan S, McShane MJ (2014) Poly (vinylsulfonic acid) assisted synthesis of aqueous solution stable vaterite calcium carbonate nanoparticles. *J Colloid Interf Sci* 418:366–372 doi: 10.1016/j.jcis.2013.12.008
26. Rodriguez-Blanco JD, Shaw S, Benning LG (2011) The kinetics and mechanisms of amorphous calcium carbonate (ACC) crystallization to calcite, via vaterite. *Nanoscale* 3:265–271 doi: 10.1039/C0NR00589D
27. Shivkumara C, Singh P, Gupta A, Hegde M (2006) Synthesis of vaterite CaCO_3 by direct precipitation using glycine and L-alanine as directing agents. *Mater Res Bull* 41:1455–1460 doi: 10.1016/j.materresbull.2006.01.026
28. Song K, Jang YN, Kim W, Lee MG, Shin D, Bang JH, Jeon CW, Chae SC (2012) Precipitation of calcium carbonate during direct aqueous carbonation of flue gas desulfurization gypsum. *Chem Eng J* 213:251–258 doi: 10.1016/j.cej.2012.10.010
29. Song K, Kim W, Park S, Bang JH, Jeon CW, Ahn JW (2016) Effect of polyacrylic acid on direct aqueous mineral carbonation of flue gas desulfurization gypsum. *Chem Eng J* 301:51–57 doi:10.1016/j.cej.2016.04.142
30. Svenskaya YI, Fattah H, Inozemtseva OA, Ivanova AG, Shtykov SN, Gorin DA, Parakhonskiy BV (2017) Key parameters for size- and shape-controlled synthesis of vaterite particles. *Cryst Growth Des* 18:331–337 doi: 10.1021/acs.cgd.7b01328
31. Svenskaya YI, Fattah H, Inozemtseva OA, Ivanova AG, Shtykov SN, Gorin DA, Parakhonskiy BV (2018) Key parameters for size- and shape-controlled synthesis of vaterite particles. *Cryst Growth Des* 18:331–337 doi:10.1021/acs.cgd.7b01328
32. Svenskaya YI, Fattah H, Zakharevich A, Gorin DA, Sukhorukov GB, Parakhonskiy B (2016) Ultrasonically assisted fabrication of vaterite submicron-sized carriers. *Adv Powder Technol* 27:618–624 doi: 10.1016/j.apt.2016.02.014
33. Tan WY, Gu Sp, Xia W, Li YX, Zhang ZX (2018) Feature changes of mercury during the carbonation of FGD gypsum from different sources. *Fuel* 212:19–26 doi: 10.1016/j.fuel.2017.09.119

34. Tolba E, Müller WE, El-Hady BMA, Neufurth M, Wurm F, Wang S, Schröder HC, Wang X (2016) High biocompatibility and improved osteogenic potential of amorphous calcium carbonate/vaterite. *J Mater Chem B* 4:376–386 doi: 10.1039/C5TB02228B
35. Tong H, Ma W, Wang L, Wan P, Hu J, Cao L (2004) Control over the crystal phase, shape, size and aggregation of calcium carbonate via a L-aspartic acid inducing process. *Biomaterials* 25:3923–3929 doi:10.1016/j.biomaterials.2003.10.038
36. Walia MK, Dick WA (2018) Selected soil physical properties and aggregate-associated carbon and nitrogen as influenced by gypsum, crop residue, and glucose. *Geoderma* 320:67–73 doi: 10.1016/j.geoderma.2018.01.022
37. Wang B, Pan Z, Cheng H, Chen Z, Cheng F (2018) High-yield synthesis of vaterite microparticles in gypsum suspension system via ultrasonic probe vibration/magnetic stirring. *J Cryst Growth* 492:122–131 doi: 10.1016/j.jcrysgro.2018.02.021
38. Wang B, Pan Z, Cheng H, Zhang Z, Cheng F (2021) A review of carbon dioxide sequestration by mineral carbonation of industrial byproduct gypsum. *J Clean Prod* 302:126930. doi: 10.1016/j.jclepro.2021.126930
39. Wang B, Pan Z, Du Z, Cheng H, Cheng F (2019) Effect of impure components in flue gas desulfurization (FGD) gypsum on the generation of polymorph CaCO_3 during carbonation reaction. *J Hazard Mater* 369:236–243 doi: 10.1016/j.jhazmat.2019.02.002
40. Wightman R, Wallis S, Aston P (2018) Leaf margin organisation and the existence of vaterite-producing hydathodes in the alpine plant *Saxifraga scardica*. *Flora* 241:27–34 doi: 10.1016/j.flora.2018.02.006
41. Xie AJ, Shen YH, Zhang CY, Yuan ZW, Zhu XM, Yang YM (2005) Crystal growth of calcium carbonate with various morphologies in different amino acid systems. *J Cryst Growth* 285:436–443 doi:10.1016/j.jcrysgro.2005.08.039
42. Xu Y, Ma G, Wang M (2014) Fabrication and growth mechanism of pumpkin-shaped vaterite hierarchical structures. *Cryst Growth Des* 14:6166–6171 doi: 10.1021/cg501477u
43. Zhao S, Duan Y, Lu J, Gupta R, Pudasainee D, Liu S, Liu M, Lu J (2018) Thermal stability, chemical speciation and leaching characteristics of hazardous trace elements in FGD gypsum from coal-fired power plants. *Fuel* 231:94–100 doi: 10.1016/j.fuel.2018.05.067
44. Zhou GT, Yao QZ, Fu SQ, Guan YB (2010) Controlled crystallization of unstable vaterite with distinct morphologies and their polymorphic transition to stable calcite. *Eur J Mineral* 22:259–269 doi: 10.1127/0935-1221/2009/0022-2008
45. Zou Z, Bertinetti L, Politi Y, Fratzl P, Habraken W (2017) Control of polymorph selection in amorphous calcium carbonate crystallization by poly(aspartic acid): two different mechanisms. *Small* 13:1603110. doi:10.1002/sml.201603100

Figures

Figure 1

(a) XRD pattern of CaCO_3 and (b) the content of vaterite and calcite in the samples obtained at different concentration of glycine. Note a mixture a calcite and vaterite are obtained in the presence of glycine, but the content of vaterite increased with glycine concentration first and then kept a constant value.

Figure 2

(a) Electrospray ionization mass spectrometry of filtrate, (b) X-ray Diffraction pattern and (c) Scanning electron microscope image of samples obtained from the reaction of calcium glycinate and CO_2 with ammonia. Note the intermediate $\text{Ca}(\text{NH}_2\text{CH}_2\text{COO})_2$ was formed during carbonation. $\text{Ca}(\text{NH}_2\text{CH}_2\text{COO})_2$ played an important role in the formation of vaterite.

Figure 3

Change in (a) pH with reaction time, (b) X-ray diffraction patterns, and (c-h) Scanning electron microscope images of products obtained from reaction of filtrate with CO_2 at different time of 3, 6, 9, 12, 15, and 24 min, respectively. Note the pH value quickly dropped first, and then kept a constant value of 7.5. Vaterite gradually formed and dominated in products from reaction of filtrate with CO_2 at different time.

Figure 4

Schematic diagram of induction mechanism of glycine for promoting formation of vaterite by CO_2 mineralization of FGDG. Note the calcite was formed through CO_3^{2-} combined with dissociative Ca^{2+} , while vaterite was generated by CO_3^{2-} combined with Ca^{2+} that bound to $\text{H}_2\text{NCH}_2\text{COO}^-$ to form vaterite CaCO_3 .

Supplementary Files

This is a list of supplementary files associated with this preprint. Click to download.

- [SupplementarymaterialEnvironmentalChemistryLetters.docx](#)